Linear, Parameter Varying Model Reduction for Aeroservoelastic Systems

Claudia P. Moreno,[*] Peter Seiler[†] and Gary J. Balas[‡]

University of Minnesota, Minneapolis, Minnesota, 55455

This paper applies a model reduction method for linear parameter-varying (LPV) systems based on parameter-varying balanced realization techniques to a body freedom flutter (BFF) vehicle. The BFF vehicle has a coupled short period and first bending mode with additional structural bending and torsion modes that couple with the rigid body dynamics. These models describe the BFF vehicle dynamics with considerable accuracy, but result in high-order state space models which make controller design extremely difficult. Hence, reduced order models for control synthesis are generated by retaining a common set of states across the flight envelope. Initially the full order BFF models of 148 states are reduced to 43 states using standard truncation and residualisation techniques. The application of balanced realization techniques at individual point designs result in 20 state models. Unfortunately, the application of balanced realization techniques at individual operating conditions results in different states being eliminated at each operating condition. The objective of LPV model reduction is to further reduce the model state order across the flight envelope while retaining consistent states in the LPV model. The resulting reduced order LPV models with 26 states capture the dynamics of interest and can be used in the synthesis of active flutter suppression controllers.

Nomenclature

A	State matrix
B	Input matrix
C	Output state matrix
D	Input feedthrough matrix
ρ	Time varying parameter vector
x	State vector
u	Input vector
T	Linear state transformation
W_C	Controllability Gramian
W_O	Observability Gramian
P	Generalized controllability Gramian
Q	Generalized observability Gramian

I.   Introduction

Modern aircraft designers are adopting light-weight, high aspect ratio wings to take advantage of wing flexibility for increased maneuverability. Those modifications can lead to improve performance and reduce operating cost. However, the high flexibility and significant deformation in flight exhibited by these aircraft increase the interaction between the rigid body and structural dynamics modes, resulting in *Body Freedom Flutter*. This phenomenon occurs as the aicraft short period mode frequency increases with airspeed and

---

[*]Graduate Research Assistant, Department of Aerospace Engineering and Mechanics.
[†]Assistant Professor, Department of Aerospace Engineering and Mechanics, and AIAA Member.
[‡]Professor and Department Head, Department of Aerospace Engineering and Mechanics, and AIAA Member.

comes close to a wing vibration mode, typically the wing bending mode. This leads to poor handling qualities and may even lead to dynamic instability. Hence, an integrated active approach to flight control, flutter suppression and structural mode attenuation is required to meet the desired handling quality performance for modern flexible aircraft.

Several flutter suppression control strategies have been proposed to address the coupled rigid body and aeroelastic dynamics including optimal control,[1,2] dynamic inversion control,[3] robust multivariable control,[4] predictive control[5] and gain scheduled control.[6,8,10] Almost all of these control strategies are model based and require accurate aerodynamic and structural dynamic models of the aircraft. Numerous investigations have addressed the aeroelastic modeling for highly flexible aircraft.[1,3,9] Modeling of a flexible aircraft requires a geometric structural model coupled with a consistent aerodynamic model. Linear aeroelastic models are based on structural finite elements and lifting-surface theory, both of which are available in general purpose commercial codes.[11] Unsteady aerodynamics are often modeled using the doublet lattice method, which results in a matrix of linear aerodynamic influence coefficients that relate the pressure change of an aerodynamic degree-of-freedom. The fully coupled, nonlinear aircraft model is a combination of the mass and stiffness matrices derived from the aeroelastic model and the unsteady aerodynamics.

Unfortunately, the inclusion of structural dynamic and aeroelastic effects result in linear, dynamic models with a large number of degrees-of-freedom defined across the flight envelope. It is unrealistic to use these high order, complex models for control design since modern control methods will result in controllers with very high state order. Even more, practical implementation of high order controllers is usually avoided since numerical errors may increase and the resulting system may present undesired behavior. Hence, a reduced-order linear model of the flexible aircraft will allow model-based multivariable controllers to be synthesized.

Several model reduction techniques for linear, parameter-varying (LPV) systems have been reported in the literature. Balanced truncation,[12] LMIs,[13] bounded parameter variaton rates,[14] coprime factorizations[17,18] and singular perturbation[15,16] are presented as an extension of the model reduction techniques for linear time invariant (LTI) systems. We plan to investigate in this paper the LPV model reduction based on coprime factorizations presented in Wood,[18] and singular perturbation scheme proposed by Widowati.[16] This paper describes the development of a low order, control-oriented aircraft model whose states are consistent across the flight envelope which is useful for intuition and also ensure easily schedule of the controllers. A balancing state transformation matrix is obtained using the generalized controlability and observability Gramians.[17,18] This approach is applied to an experimental body freedom flutter test vehicle model developed by the U.S Air Force described in section II. Comparison between balanced reduction methods for unstable LTI systems[19,20] and the proposed method are presented in section IV.

II.   Body Freedom Flutter Model

The Air Force Research Laboratory (AFRL) contracted with Lockheed Martin works to develop a flight test vehicle, denoted Body Freedom Flutter (BFF) vehicle, to demonstrate active aeroelastic control technologies. The vehicle is a high aspect ratio flying wing with light weight airfoil. Details of the vehicle's design can be found in Beranek.[21] The aircraft configuration with the location of accelerometers and control surfaces for flutter suppression is presented in the Fig. 1.

The aeroservoelastic (ASE) model of the BFF vehicle was assembled using MSC/NASTRAN.[11] The initial structural model was created with 2556 degrees-of-freedom and then reduced to 376 degrees-of-freedom via a Guyan reduction. A Ground Vibration Test was performed to validate the structural model and six critical modes were found. Table 1 lists the mode shapes and frequency values of the structural model.[22] The aerodynamics were modeled using the doublet lattice method which is a technique to model oscillating lifting surfaces. This model produces a matrix of linear aerodynamic influence coefficients that describes the pressure change of the 2252 aerodynamic degrees-of-freedom. The mass, stiffness and aerodynamic coefficient matrices are combined using the P-K method which interconnects the structural and aerodynamic grids by splinning interpolation and finds the generalized aerodynamic matrix using the structural modal matrix.[11] The unsteady aerodynamics is approximated with a rational function to create a continuous-time aeroservoelastic state-space model of the airframe with 148 states. The general state-space form of the model is given by
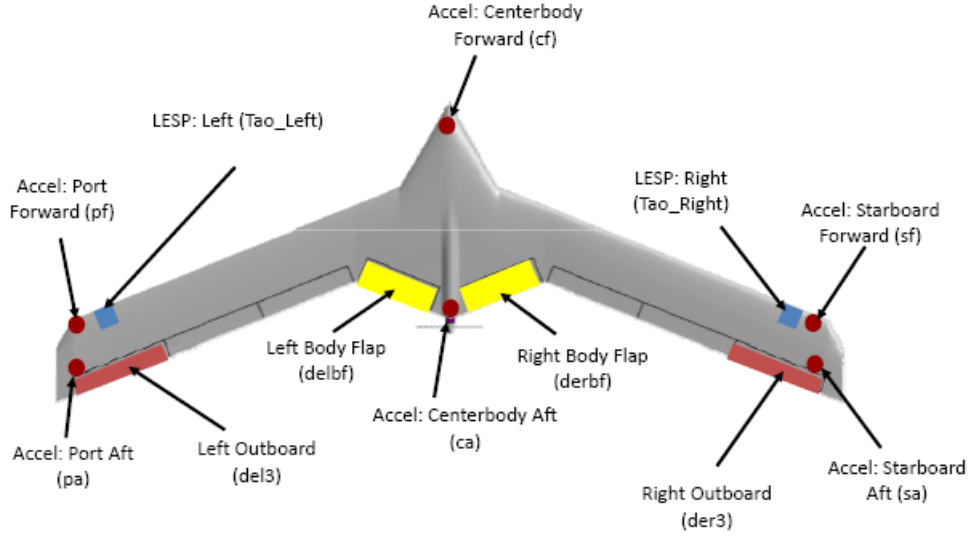
American Institute of Aeronautics and Astronautics

Figure 1. Body Freedom Flutter Vehicle[22]

Table 1. Ground Vibration Test Frequencies

Mode Shape	Frequency (rad/s)
Symmetric Wing 1st Bending	35.37
Anti-symmetric Wing 1st Bending	54.98
Symmetric Wing 1st Torsion	123.34
Anti-symmetric Wing 1st Torsion	132.76
Symmetric Wing 2nd Bending	147.28
Anti-symmetric Wing 2nd Bending	185.73

$$\begin{Bmatrix} \dot{x}_p \\ \dot{x}_q \\ \dot{x}_{\omega 1} \\ \dot{x}_{\omega 2} \end{Bmatrix} = \begin{bmatrix} 0 & I & 0 & 0 \\ A_{21} & A_{22} & A_{23} & A_{24} \\ 0 & I & \omega_1 I & 0 \\ 0 & I & 0 & \omega_2 I \end{bmatrix} \begin{Bmatrix} x_p \\ x_q \\ x_{\omega 1} \\ x_{\omega 2} \end{Bmatrix} + \begin{bmatrix} B_1 \\ B_2 \\ 0 \\ 0 \end{bmatrix} u \tag{1}$$

Eq. (1) represents a typical second order equation of motion with augmented state vector due to the rational functions approximation. The state vector consists of modal displacements, x_p, modal velocities, x_q, and two lags states, $x_{\omega 1}$, $x_{\omega 2}$, for the unsteady aerodynamic rational function approximation. Moreover, each of the set of states is related with 5 rigid body modes (lateral, plunge, roll, pitch and yaw), 8 flexible modes (symmetric - anti-symmetric bending and torsion) and 24 secondary discrete degrees-of-freedom.

Finally, a set of state space matrices was generated in 2 knot increments from 40 to 90 KEAS (knots equivalent airspeed) with variable Mach at constant altitude of 3000 ft.[22] Transfer function magnitudes from the right body flap (drbfc) and right wing outboard flap (drwfoc) to the pitch rate (QbDps) and vertical accelerometer in the right wing (NzRWtipAftG) for three flight conditions are plotted in the Fig. 2. The frequency and damping of the critical modes for the BFF vehicle are plotted at Fig. 3 as a function or airspeed.

Plots show how the model dynamics changes dramatically as function of airspeed. Coupling of the short period with the symmetric wing bending produces BFF at 43 KEAS with a frequency of 24.3 rad/s. Flutter is also presented when the symmetric wing bending and torsion modes are coupled at an airspeed of 58 KEAS with frequency of 65 rad/s and when the anti-symmetric wing bending and torsion modes comes close
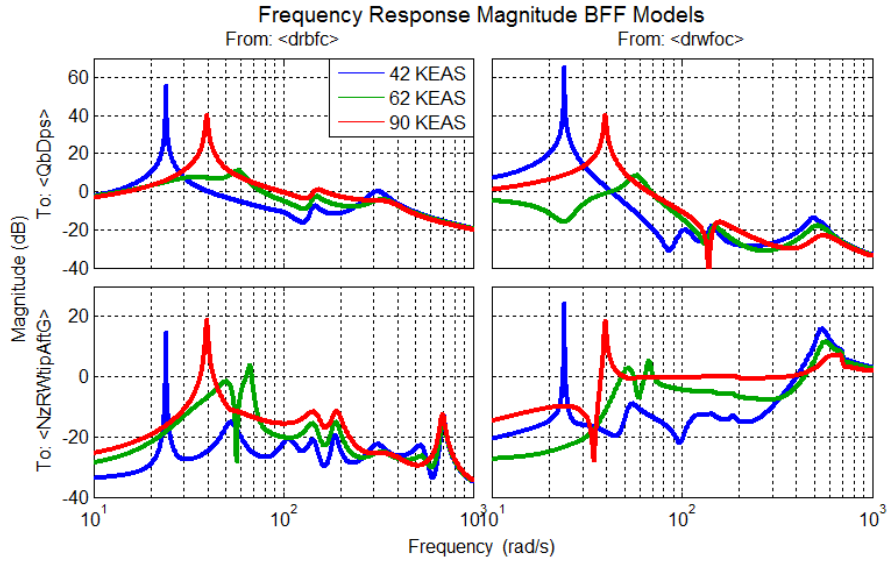
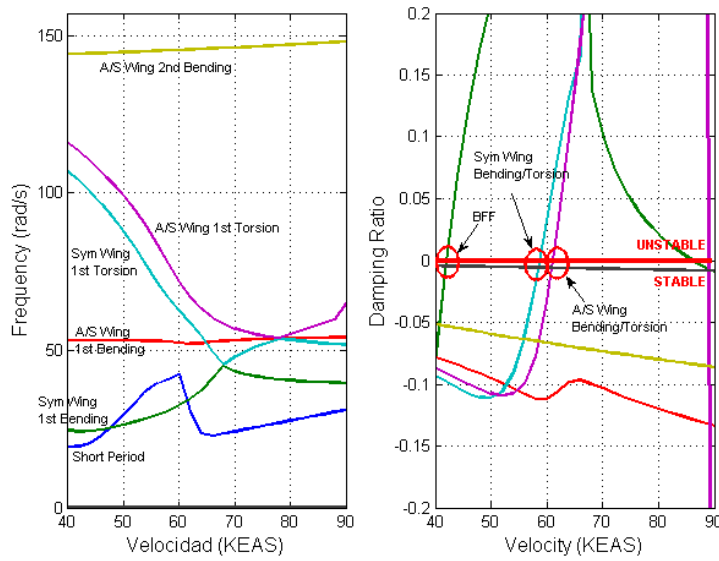**Figure 2. Frequency response magnitudes of BFF model at 42, 62 and 90 KEAS**

Figure 3. Velocity/frequency/damping plot for BFF vehicle

in proximity at 61 KEAS with frequency of 69 rad/s. Hence, the flight envelope of the open-loop vehicle is limited till 42 KEAS before the vehicle becomes unstable.

III.   Classical Model Reduction

The linear, coupled state-space models of the vehicle generated across the flight envelope are function of the dynamic pressure and Mach. These state space models can be written as

$$
\left\{ \begin{array}{c} \dot{x}(t) \\ y(t) \end{array} \right\} = \left[\begin{array}{cc} A(\rho) & B(\rho) \\ C(\rho) & D(\rho) \end{array} \right] \left\{ \begin{array}{c} x(t) \\ u(t) \end{array} \right\} \tag{2}
$$

American Institute of Aeronautics and Astronautics

Where $A(\rho)$ is the state matrix, $B(\rho)$ is the input matrix, $C(\rho)$ is the output state matrix, $D(\rho)$ is the input feedthrough matrix and ρ is a vector that is function of time and corresponds to dynamic pressure and Mach for the BFF model. This model is called a *linear parameter-varying* (LPV) system.

Typically, LPV ASE models result in high-order state-space models. High-order controllers can be obtained using these complex models but, the implementation of these high-order state controllers is usually avoided because numerical errors may generate undesirable behavior in the system. Hence, reduced-order LPV models are required for controller synthesis. Traditional reduction techniques for linear time invariant systems have been extended to LPV systems.[12–15, 17] However, Eq. (3) shows that the state transformation used depends on ρ, and in general it would be time-varying. This transformation $T(\rho)$ would introduce additional terms, that depend on the derivative of $T(\rho)$ with respect to time, in the state space model making the reduction problem harder. Hence, a model reduction technique that preserves the same state meaning across the flight envelope with an invariant state transformation is presented. This approach is useful for retaining physical intuition and will ensure that the resulting LPV model does not increase in complexity.

$$
\begin{aligned}
x_c &= T(\rho)x \Rightarrow \dot{x}_c = \dot{\rho}\dot{T}(\rho)\dot{x} \\
\dot{x}_c &= \dot{\rho}\dot{T}(\rho)A(\rho)T^{-1}(\rho)x_c + \dot{\rho}\dot{T}(\rho)B(\rho)u \\
y &= C(\rho)T^{-1}(\rho)x_c + D(\rho)u
\end{aligned}
\tag{3}
$$

The model reduction goal is to reduce the complexity of models while preserving their input-output behavior. The main idea is to eliminate the states with little contribution to the energy transferred from the input to the output. Partitioning the state vector x, into $[x_1, x_2]^T$, where x_2 contains the states to remove, the state-space equations become:

$$
\begin{aligned}
\dot{x}_1 &= A_{11}x_1 + A_{12}x_2 + B_1u \\
\dot{x}_2 &= A_{21}x_1 + A_{22}x_2 + B_2u \\
y &= C_1x_1 + C_2x_2 + Du
\end{aligned}
\tag{4}
$$

This notation will be used in the next subsections to indicate the different model reduction techniques applied.

A. Truncation

The focus of the control design is to actively control flutter and vehicle/wing vibration. Fig. 3 shows flutter phenomena occuring in a frequency bandwith between 10-120 rad/s across the flight envelope, hence the extremely slow dynamics can be eliminated from the model. The plunge mode of the BFF vehicle turns out to be very slow comparing with flutter frequencies. Hence, the state corresponding to the plunge mode is truncated retaining the system behavior at infinity frequency. The reduced model with 147 states is given by

$$
\begin{aligned}
\dot{x}_1 &= A_{11}x_1 + B_1u \\
y &= C_1x_1 + Du
\end{aligned}
\tag{5}
$$

B. Residualization

Residualization takes into account the interaction between slow and fast dynamics while preserving the physical nature of the state variables. This is accomplished by having the degrees of freedom to be removed from the model reach their steady state values instantaneously, this corresponds to setting the derivatives of the fast states to zero. For a general system with the space state structure in Eq. (4), the solution for the reduced model is given by

$$
\begin{aligned}
\dot{x}_1 &= (A_{11} - A_{12}A_{22}^{-1}A_{21})x_1 + (B_1 - A_{12}A_{22}^{-1}B_2)u \\
y &= (C_1 - C_2A_{22}^{-1}A_{21})x_1 + (D - C_2A_{22}^{-1}B_2)u
\end{aligned}
\tag{6}
$$

American Institute of Aeronautics and Astronautics

States are residualized based on the physics of the vehicle. The lateral and yaw rigid body modes, the symmetric wing fore and aft, anti-symmetric wing 2nd bending and rotation modes and 18 discrete degrees-of-freedom in the actuators for all the control surfaces, are residualized. Additionally, the derivatives and aerodynamic lags corresponding to the same states are also residualized. As result, 92 states are eliminated from each LTI model and reduced models with 55 states are obtained across the flight envelope.

C.   Modal Residualization

A modal residualization is performed in order to eliminate high frequencies outside the bandwidth of interest that were retained after the truncation and residualization procedures. A single modal transformation is applied to the models in order to preserve states across the flight envelope. A state coordinate transformation, T, is used to find a modal realization such that

$$
\begin{aligned}
x_c &= Tx \\
\dot{x}_c &= TAT^{-1}x_c + TBu \\
y &= CT^{-1}x_c + Du
\end{aligned}
\tag{7}
$$

A single transformation for the BFF vehicle is computed using the residualized model at 84 KEAS for which the minimum errors were found. A total of 12 high frequency modes were residualized and reduced models with 43 states are obtained across the flight envelope. Fig. 4 and Fig. 5 show the comparison between the original airframe model with 148 states and the reduced model with 43 states at three different flight conditions. Figures show the frequency responses from the right body flap (drbfc) and right wing outboard flap (drwfoc) to the pitch rate (QbDps) and vertical accelerometer in the right wing (NzRWtipAftG) are plotted to compare the reduced models and the original models.
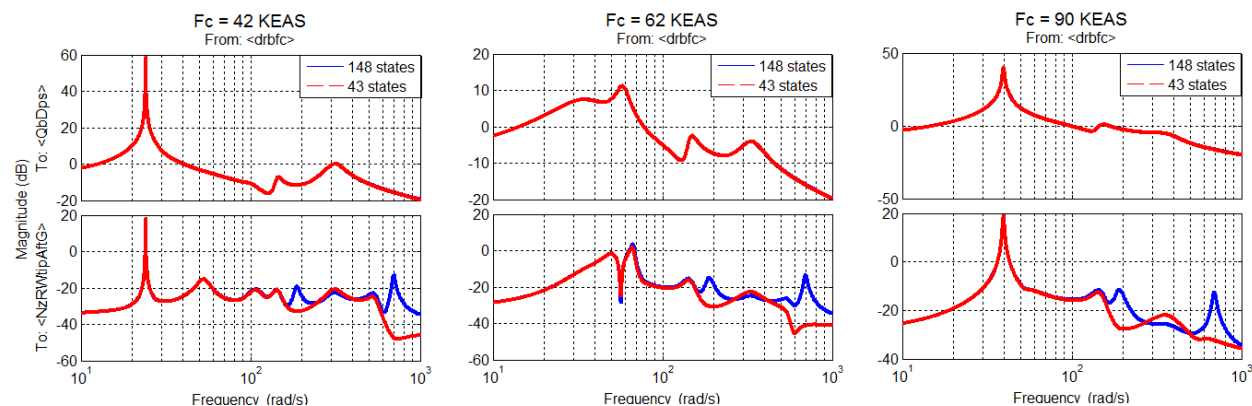

Figure 4.   Frequency response of the BFF airframe model (blue) and modal residualization model (red) from right body flap to pitch rate and right wing accelerometer

The relative error between the 148 states model and the 43 states model obtained after applying the classical model reduction methods is plotted in Fig. 6 for flight conditions at 42, 62 and 90 KEAS. Additionally, Fig. 7 shows the norm of these errors across the flight envelope. It is observed that in general the differences between models are less than 10% for all the flight conditions except for the models at 42 and 86 KEAS where the maximum difference is around 50%. These significant difference in the models at particular frequencies are due to highly undamped modes that the reduced models cannot capture completely.

IV.   Balanced Reduction for Unstable Systems

Balanced reduction is based on the measure of the controllability and observability in certain directions of the state space model. These measures are given by the controllability and observability Gramians defined, respectively, as
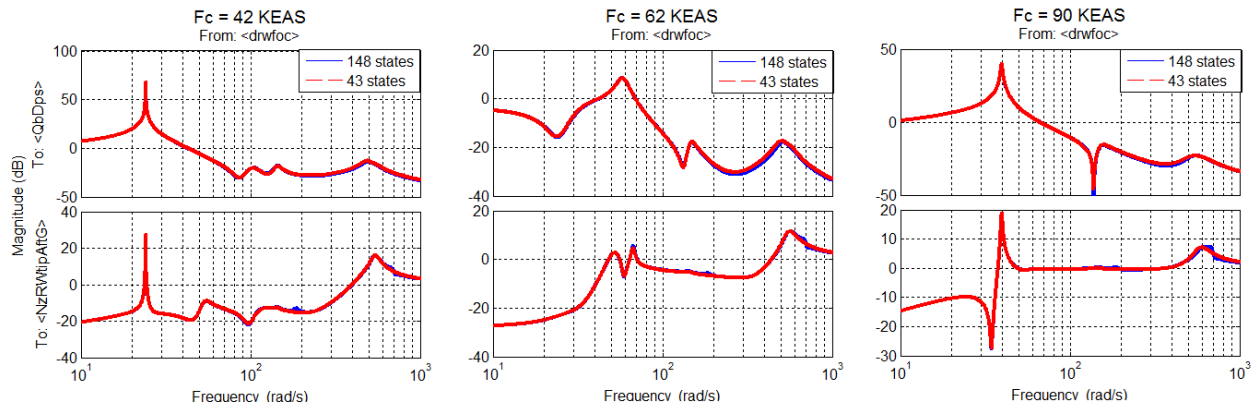
American Institute of Aeronautics and Astronautics

Figure 5. Frequency response of the BFF airframe model (blue) and modal residualization model (red) from right wing outboard flap to pitch rate and right wing accelerometer
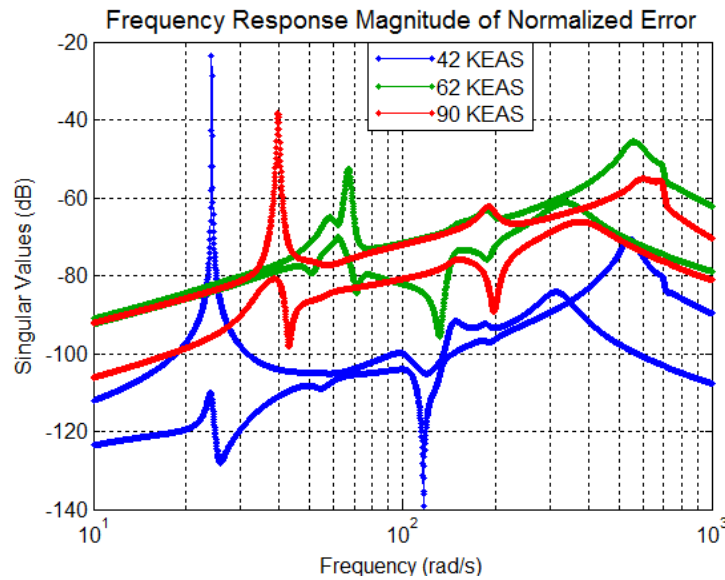

Figure 6. Frequency response of the difference between the BFF airframe model and modal residualization model for flight conditions at 42, 62 and 90 KEAS

$$W_C = \int_0^\infty e^{At} BB^T e^{A^T t} dt \tag{8}$$

$$W_O = \int_0^\infty e^{A^T t} C^T C e^{At} dt \tag{9}$$

Solutions to these integrals are also the solutions to the following Lyapunov equations:

$$AW_C + W_C A^T + BB^T = 0 \tag{10}$$

$$A^T W_O + W_O A + C^T C = 0 \tag{11}$$

A balanced realization of a system is a realization with equal and diagonal controllability and observability Gramians, $\hat{P} = \hat{Q} = \Sigma$. Hence, the balancing state transformation, T, is chosen such that $\hat{W}_c = TW_c T^* = \Sigma$ and $\hat{W}_o = (T^{-1})^* W_o T^{-1} = \Sigma$ and also, gives the eigenvector decomposition of the product of the Gramians $W_C W_O = T^{-1} \Lambda T$.
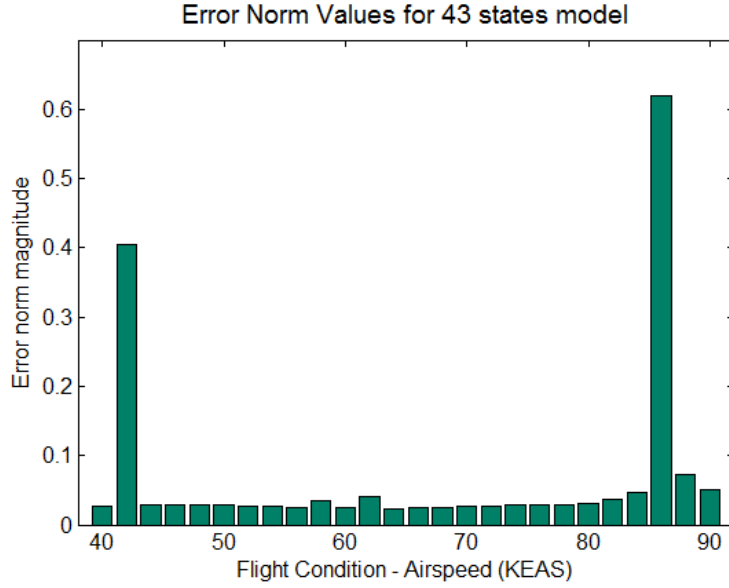
American Institute of Aeronautics and Astronautics

Figure 7. Norm error values across the flight envelope for reduced model with 43 states

Unfortunately, the controllability and observability Gramians given by Eq. (8) and Eq. (9) are not defined for unstable systems since the integrals will be unbounded when the matrix A is unstable. The standard approaches to balanced reduction require the nominal system to be stable. Since aeroservoelastic models are mixed stability systems, a balanced model reduction technique which handles stable and unstable modes in the same framework would offer an opportunity to find a single balancing transformation across the flight envelope and retain a consistent set of states at each flight condition.

A. LTI Unstable Systems

Several methods have been proposed to find balancing transformations for unstable systems.[18–20] Therapos[19] shows that an unstable system can be balanced if and only if the product of the controllability, observability Gramians is similar to a diagonal matrix. Here, the controllability and observability Gramians are calculated as the solutions for the Lyapunov equations (10) and (11) deriving the necessary and sufficient conditions for their existence. Using this method with the BFF models, we find a balancing transformation at a particular flight condition and apply it to the models across the flight envelope. Results show that the balancing transformation computed at 76 KEAS obtains models with 32 states across the flight envelope with acceptable errors.

Zhou[20] proposed the generalization of the controllability and observability Gramians using a frequency domain characterization, separating the stable and unstable part of the system and balancing both parts separately. The controllability and observability Gramians are described as

$$P = \int_{-\infty}^{\infty} \frac{1}{2\pi} (j\omega I - A)^{-1} BB^T (j\omega I - A^T)^{-1} d\omega \tag{12}$$

$$Q = \int_{-\infty}^{\infty} \frac{1}{2\pi} (-j\omega I - A^T)^{-1} C^T C (j\omega I - A)^{-1} d\omega \tag{13}$$

Using a linear transformation to separate the stable and unstable part of the system such that

$$\left[\begin{array}{c|c} TAT^{-1} & TB \\ \hline CT^{-1} & D \end{array} \right] = \left[\begin{array}{cc|c} A_1 & 0 & B_1 \\ 0 & A_2 & B_2 \\ \hline C_1 & C_2 & D \end{array} \right] \tag{14}$$

American Institute of Aeronautics and Astronautics

Where A_1 is the stable part and A_2 the antistable part. The generalized controllability and observability Gramians are, respectively

$$P = T^{-1} \begin{bmatrix} P_1 & 0 \\ 0 & P_2 \end{bmatrix} (T^{-1})^T \tag{15}$$

$$Q = T^T \begin{bmatrix} Q_1 & 0 \\ 0 & Q_2 \end{bmatrix} T \tag{16}$$

Being P_1 and Q_1 the controllability and observability Gramians of (A_1, B_1, C_1) and P_2 and Q_2 the Gramians of $(-A_2, B_2, C_2)$. The method is applied to the BFF model obtaining reduced models with 32 states across the flight envelope. Here, the balancing transformation is obtained using the Gramians for the flight condition at 84 KEAS. Error bounds for all the models are acceptable having the tendency to increase as the airspeed decreases. In addition, a point balanced reduction is performed for each flight condition. Using the corresponding transformation for each flight condition, the models can be reduced until 20 states with good accuracy but different states are eliminated at each flight condition across the flight envelope. Fig. 8 and Fig. 9 show the comparison between the BFF models with 43 states and the reduced models obtained using the LTI methods described. Frequency responses from the right body flap (drbfc) and right wing outboard flap (drwfoc) to the pitch rate (QbDps) and vertical accelerometer in the right wing (NzRWtipAftG) are plotted for the same three flight conditions as before.
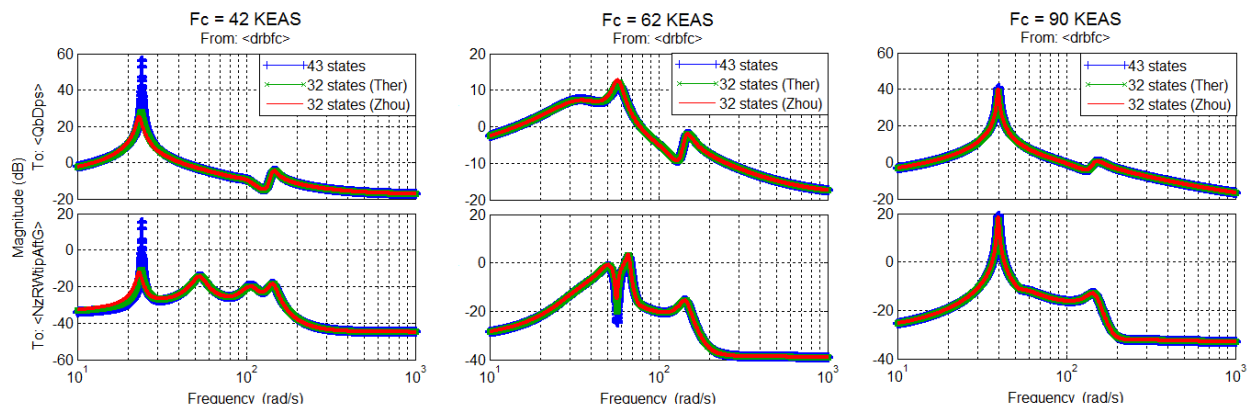

Figure 8. Frequency response of the modal residualization model (blue), Therapo's balanced model (green) and Zhou's balanced model (red) from right body flap to pitch rate and right wing accelerometer
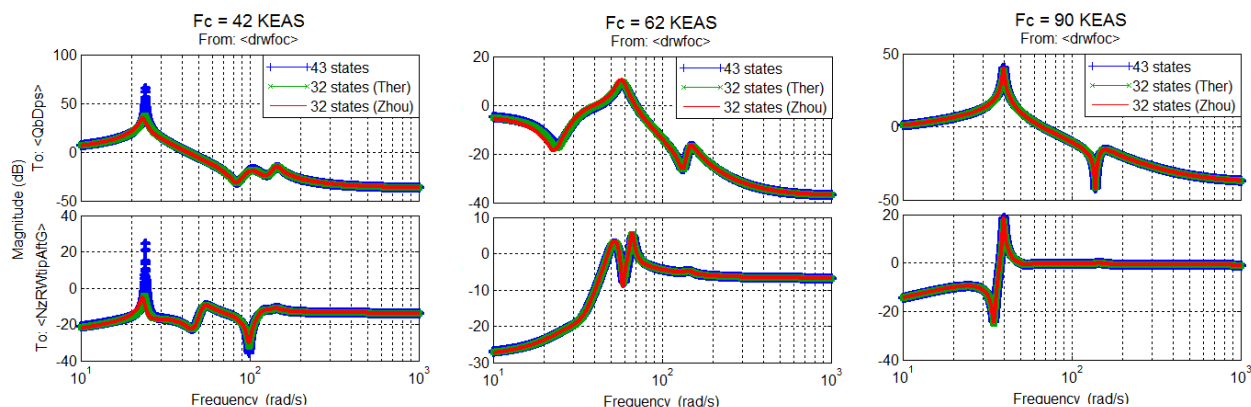

Figure 9. Frequency response of the modal residualization model (blue), Therapo's balanced model (green) and Zhou's balanced model (red) from right wing outboard flap to pitch rate and right wing accelerometer

American Institute of Aeronautics and Astronautics

The relative errors between the 43 states model and the 32 states models obtained after applying the LTI model reduction methods with a single balancing transformation are plotted in Fig. 10 for the flight conditions at 42, 62 and 90 KEAS.
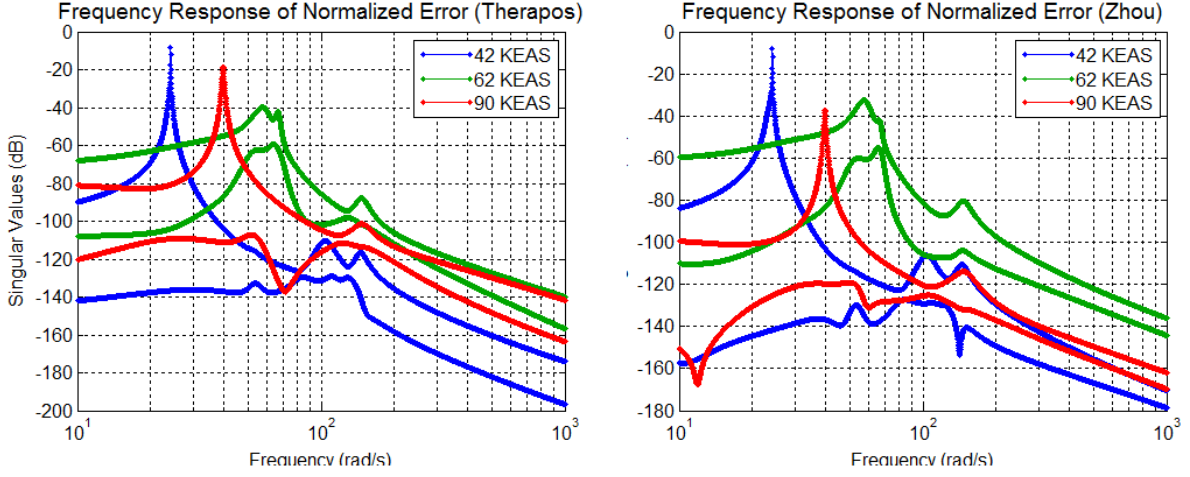

Figure 10. Frequency response of the difference between the 43 states model and 32 states models for flight conditions at 42, 62 and 90 KEAS

B.   LPV Unstable Systems

The LPV model reduction proposed in this paper is based on coprime factorizations and singular perturbation.[16, 18] The coprime factorization of LTI systems is extended to LPV systems to generate a set of all stable input-output pairs. Gramians for this coprime factorization representation are found to be related to the solutions of two Ricatti inequalities. The Generalized Control Ricatti Inequality (GCRI) and the Generalized Filtering Ricatti Inequality (GFRI), defined as

$$(A(\rho) - B(\rho)S^{-1}(\rho)D^T(\rho)C(\rho))^T X + X(A(\rho) - B(\rho)S^{-1}(\rho)D^T(\rho)C(\rho)) - \tag{17}$$
$$XB(\rho)S^{-1}(\rho)B^T(\rho)X + C^T(\rho)R^{-1}(\rho)C(\rho) < 0$$

$$(A(\rho) - B(\rho)D^T(\rho)R^{-1}(\rho)C(\rho))Y + Y(A(\rho) - B(\rho)D^T(\rho)R^{-1}(\rho)C(\rho))^T - \tag{18}$$
$$YC^T(\rho)R^{-1}(\rho)C(\rho)Y + B(\rho)S^{-1}(\rho)B^T(\rho) < 0$$

where $S(\rho) = I + D^T(\rho)D(\rho)$, $R(\rho) = I + D(\rho)D^T(\rho)$, $X = X^T > 0$ and $Y = Y^T > 0$. Hence, the observability and controllability Gramians are computed, respectively

$$Q \;=\; X \tag{19}$$
$$P \;=\; (I + YX)^{-1}Y \tag{20}$$

The generalized observability and controllability Gramians are calculated for the LPV BFF model by solving a Linear Matrix Inequality representation of the GCRI and GFRI. Using Schur complement and the variables $\bar{X} = X^{-1}$ and $\bar{Y} = Y^{-1}$, the GCRI and GFRI are equilavent to the LMIs described by Eq. (21) and Eq. (22).

$$\begin{bmatrix} \bar{X}A_C^T(\rho) + A_C(\rho)\bar{X} - B(\rho)S^{-1}(\rho)B^T(\rho) & \bar{X}C^T(\rho) \\ C(\rho)\bar{X} & -R(\rho) \end{bmatrix} < 0 \tag{21}$$

$$\begin{bmatrix} \bar{Y}A_F(\rho) + A_F^T(\rho)\bar{Y} - C^T(\rho)R^{-1}(\rho)C(\rho) & \bar{Y}B(\rho) \\ B^T(\rho)\bar{Y} & -S(\rho) \end{bmatrix} < 0 \tag{22}$$

where $A_C(\rho) = A(\rho) - B(\rho)S^{-1}(\rho)D^T(\rho)C(\rho)$ and $A_F(\rho) = A(\rho) - B(\rho)D^T(\rho)R^{-1}(\rho)C(\rho)$.

The size of the LMI problem grows as function of the state order and number of parameters of the LPV system. The number of variables to solve for symmetric matrices is related with the state order as $k = n(n+1)/2$. The solution for the controllability and observability Gramians using the BFF model with 43 states involves 946 decision variables and the feasibility of 27 linear matrix inequalities. LMI constraints result from the grid models across the flight envelope and the positive definite condition for the solutions. Solutions are computed using the LMI Lab in the Robust Control Toolbox for MATLAB[24]

Reduced models with 26 states were obtained using the coprime factorization realization described in Wood[18] and the singular perturbacion approximation proposed by Widowati.[16] Fig. 11 and Fig. 12 plot the comparison between the reduced models obtained by the LPV model reduction proposed and the individual point reduction at 42, 62 and 90 KEAS. The relative error between the 43 states model and the 26 states model obtained with the LPV Gramians is plotted as function of frequency at Fig. 13. Additionally, a comparison between the 43 states model and the models resulting from the corresponding LTI balancing transformation at each flight condition is also plotted at Fig. 13. Figures show the frequency responses from the right body flap (drbfc) and right wing outboard flap (drwfoc) to the pitch rate (QbDps) and vertical accelerometer in the right wing (NzRWtipAftG) for the same three flight conditions as before.
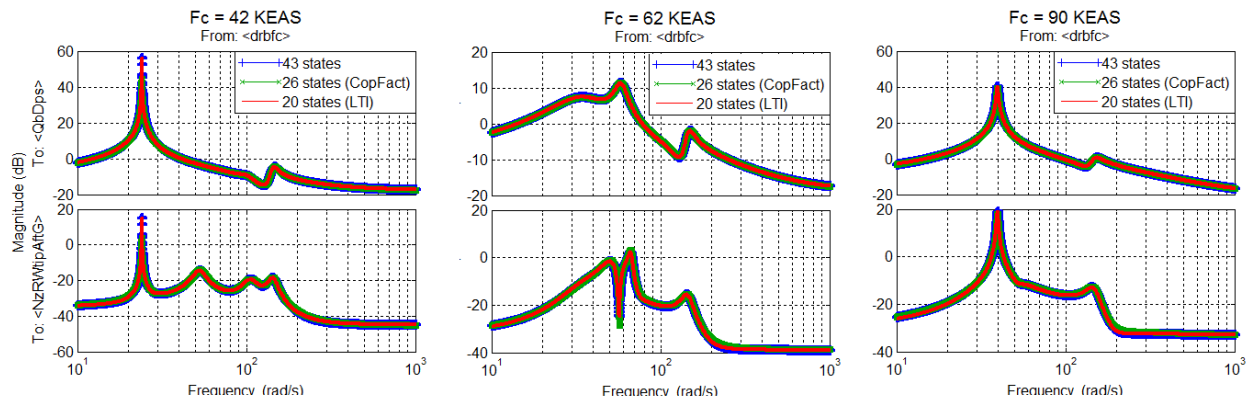

Figure 11. Frequency response of the modal residualization model (blue), Coprime Fact. balanced model (green) and LTI balanced model (red) from right body flap to pitch rate and right wing accelerometer
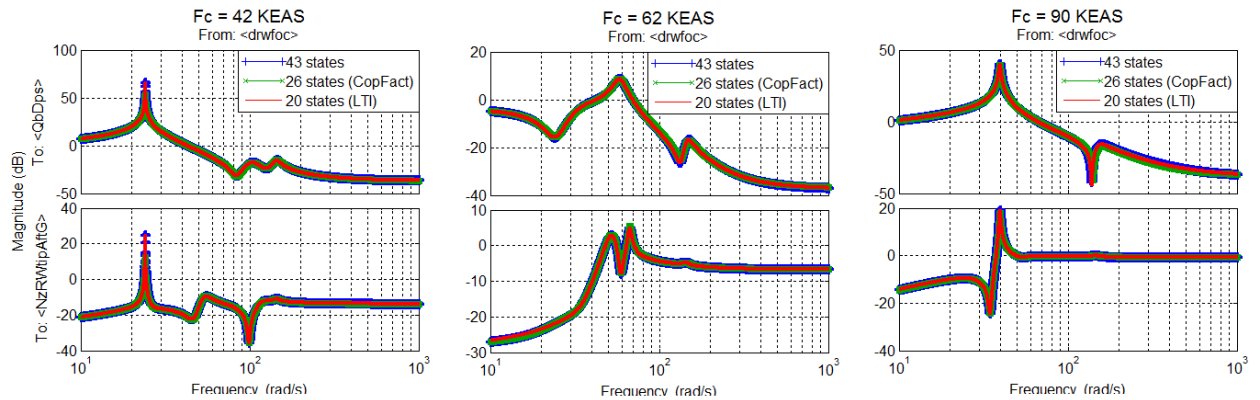

Figure 12. Frequency response of the modal residualization model (blue), Coprime Fact. balanced model (green) and LTI balanced model (red) from right wing outboard flap to pitch rate and right wing accelerometer

Error magnitudes, plotted at Fig. 14, compare the different methods evaluated. Results show that LPV reduced models with 26 states, obtained using the balancing transformation by the coprime factorization method, have errors less than 10% for almost all the flight conditions. The largest errors are again related with the flight conditions where the systems are marginally stable. Additionally, it is observed that the reduced models obtained from application of the LTI balancing transformations derived at a particular

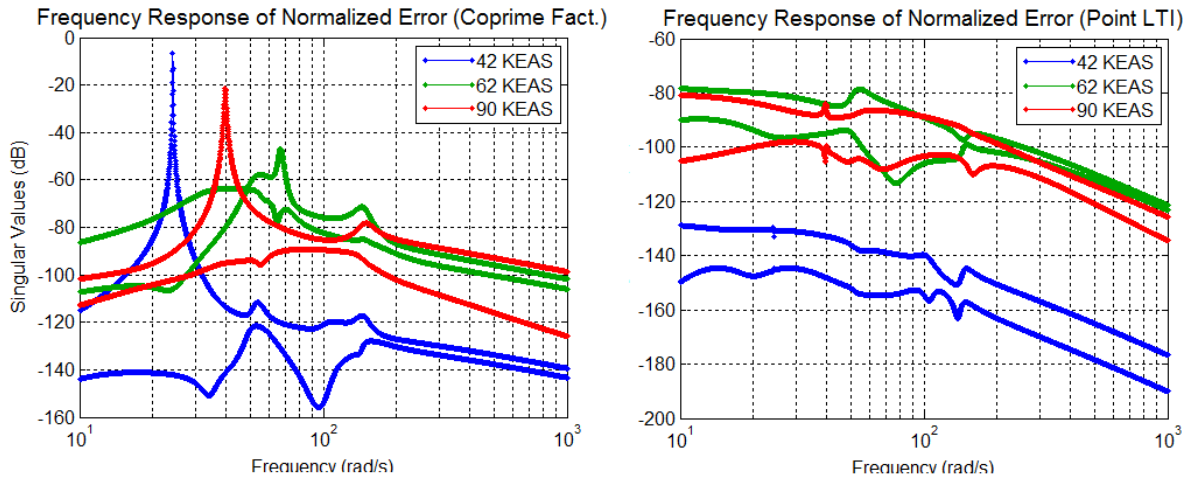American Institute of Aeronautics and Astronautics

Figure 13. Frequency response of the difference between the 43 states model, 26 states model and 20 states model for flight conditions at 42, 62 and 90 KEAS

operation point, result in higher order models than the models obtained by the LPV reduction proposed. These reduced models with 32 states result sensitive to errors as the model differs from the operation point for which the transformation was computed and differences between $40 - 80\%$ are obtained at several flight conditions. Even though, lower order models of 26 states were found using the LPV method proposed with better acurracy than the models obtained by LTI methods described before, results show that LPV reduced models are in general higher order than the reduced models obtained using the corresponding balancing transformation which varies at each flight condition. In this case, the linear models can be reduced till 20 states with very small errors as the Fig. 13 shows. These results were expected due to the dramatic change in the dynamics of the models and the desired of a consistent state vector across the flight envelope that make the reduction problem harder.
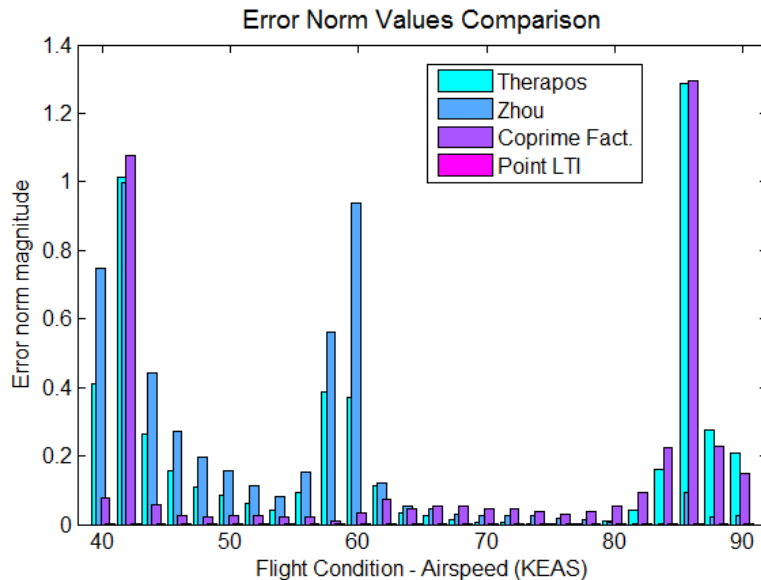

Figure 14. Norm error values across the flight envelope for balanced reduction methods

American Institute of Aeronautics and Astronautics

V.   Numerical Issues

The LMI constraints described at Eq. (21) and Eq. (22) are parameter dependent. This means that there is an infinite set of LMIs, one for each parameter value, which makes the feasibility problem hard to solve. To ensure that the inequalities are satisfied everywhere, a dense grid covering the parameter space must be created. Unfortunately, a dense grid of parameters would result in a large number of LMI constraints causing computational issues. Particularly, the LPV reduction problem proposed for the BFF vehicle is directly related with the state order of the system. Using a 43 states model to compute the generalized controllability and observability Gramians involves 946 decision variables to check at 27 LMI constraints. Solutions for the GFRI and GCRI are computed after 3396 seconds using a standard personal computer and indicate that the problem has a large size. However, the solution for the GFRI is marginally feasible which means that the feasible point computed may not satisfy the entire set of LMI constraints. Even more, finding the controllability and observability Gramians for higher order models will increase the size of the LMI problem causing numerical issues. Trying to solve the GFRI and GCRI using models with 55 states at 5 flight conditions requires 1540 decision variables for which the LMI Lab cannot find feasible solutions. Additionally, the significant change in the dynamics across the flight envelope may lead also to feasibility problems. Hence, future work related with LMI feasibility for aeroservoelastic systems is required.

VI.   Conclusion

A model reduction procedure for aeroservoelastic models based on LPV balanced realizations has been proposed. The proposed procedure is applied to a body freedom flutter (BFF) vehicle and consists of a truncation of uncoupled slow dynamics and a residualization of coupled modes outside the flutter frequencies of interest. A modal transformation is applied to all the models in order to eliminate remaining high frequency modes. The full order models with 148 states were initially reduced to 43 states using traditional order reduction techniques while retaining the main flutter dynamics and the same states characteristics across the flight envelope. Three methods to find balanced models for unstable system were tested. Low order, control-oriented aircraft models with 26 states consistent across the flight envelope were obtained using the coprime factorization and singular perturbation approach. Linear analysis of the individual point designs indicate that a lower bound for the reduced order LPV will be 20 states. The LPV reduced order model results in higher order due to the varying dynamics of the vehicle across the flight envelope, though the consistency of states across the flight envelope is useful from physical insight and it ensures easily scheduling of controllers.

Acknowledgments

References

[1]Holm-Hansen, B., Atkinson, C., Beranek, J., Burnett, E., Nicolai, L., and Youssef, H., "Envelope expansion of a flexible flying wing by active flutter suppression ", *AUVSI's Unmanned Systems North America*, Vol. 1, Denver, CO, 2010.

[2]Mukhopadhyay, V., "Flutter suppression control law design and testing for the active flexible wing ", *Journal of Aircraft*, Vol. 32, No. 1, 1995, pp. 45-51.

[3]Raghavan, B., "Flight dynamics and control of highly flexible flying-wings ", Ph.D. Dissertation, Aerospace and Ocean Engineering Dept., Virginia Polytechnic Institute and State University, Blacksburg, VA, 2009.

[4]Waszak, M., "Robust multivariable flutter suppression for the benchmark active control technology (BACT) wind-tunnel model ", *11th Symposium on Structural Dynamics and Control*, Vol. 1, Blacksburg, VA, 1997.

[5]Haley, P., and Soloway, D., "Generalized predictive control for active flutter suppression ", *IEEE Control Systems*, Vol. 17, No. 4, 1997, pp. 64-70.

[6]Balas, G. J., "Linear, parameter-varying control and its application to aerospace systems ", *23rd Congress of International Council of the Aeronautical Sciences*, ICAS 2002-5.4.1, Toronto, Canada, 2002, pp. 541.1-541.9.

[7]Barker, J. M., Balas, G. J., and Blue, P. A., "Gain-scheduled linear fractional control for active flutter suppression ", *AIAA Journal of Guidance, Dynamics and Control*, Vol. 22, No. 4, 1999, pp. 507-512.

[8]Van Etten, C., Balas, G. J., and Bennani, S., "Linear parameter-varying integrated flight and structural mode control for a flexible aircraft ", *AIAA Guidance, Navigation and Control Conference*, Portland, OR, 1999.

[9]Patil, M. J., and Hodges, D. H., "Flight dynamics and control of highly flexible flying-wings ", *Journal of Aircraft*, Vol. 43, No. 6, 2006, pp. 1790-1798.

[10]Barker, J. M., Balas, G. J., and Blue, P. A., "Gain-scheduled linear fractional control for active flutter suppression ", *AIAA Journal of Guidance, Dynamics and Control*, Vol. 22, No. 4, 1999, pp. 507-512.

[11]Rodden, W. P., and Johnson, E. H., "MSC/NASTRAN Aeroelastic Analysis User's Guide ", *MacNeal-Schwendler Corp.*, Ver. 68, 1994.

[12]Lall, S., and Beck, C., "Error-bounds for balanced model-reduction of linear time-varying systems ", *IEEE Transactions on Automatic Control*, Vol. 48, No. 6, 2003, pp. 946-956.

[13]Saragih, R., "Model reduction of linear parameter varying systems based on LMIs ", *Proceedings of the 2nd IMT-GT Regional Conference on Mathematics, Statistics and Applications*, Penang, Malasya, 2006.

[14]Widowati, R., and Bambang, R. "Model reduction of LPV control with bounded parameter variation rates ", *6th Asian Control Conference*, Bali, Indonesia, 2006.

[15]Farhood, M., and Dullerud, G. E. "Model reduction of nonstationary LPV systems ", *IEEE Transactions on Automatic Control*, Vol. 52, No. 2, 2007, pp. 181-196.

[16]Widowati, R., Bambang, R., Sagari, R. and Nababan, S. M. "Model reduction for unstable LPV system based on coprime factorizations and singular perturbation ", *5th Asian Control Conference*, Vol. 2, Melbourne, Australia, 2004, pp. 963-970.

[17]Wood, G. D., "Control of parameter-dependent mechanical systems ", Ph.D. Dissertation, Aerospace and Ocean Engineering Dept., Cambridge University, Cambridge, UK, 1995.

[18]Wood, G. D., Goddard, P. J., and Glover, K., "Approximation of Linear Parameter-Varying Systems ", *Proceedings of the 35th IEEE Conference on Decision and Control*, Vol. 4, Kobe, Japan, 1996, pp. 406-411.

[19]Therapos, C., "Balancing transformations for unstable nonminimal linear systems ", *IEEE Transactions on Automatic Control*, Vol. 34, No. 4, 1989, pp. 455-457.

[20]Zhou, K., Salomon, G., and Wu, E., "Balanced realization and model reduction for unstable systems ", *International Journal of Robust and Nonlinear Control*, Vol. 9, No. 3, 1999, pp. 183-198.

[21]Beranek, J., Nicolai, L., Buonanno, M., Burnett, E., Atkinson, C., Holm-Hansen, B. and Flick, P., "Conceptual design of a multi-utility aeroelastic demonstrator ", *13th AIAA/ISSMO Multidisciplinary Analysis Optimization Conference*, Vol. 3, Fort Worth, TX, 2010, pp. 2194-2208

[22]Burnett E., Atkinson, C., Beranek, J., Sibbitt, B., Holm-Hansen, B. and Nicolai, L., "NDOF Simulation model for flight control development with flight test correlation ", *AIAA Modeling and Simulation Technologies Conference*, Vol. 3, Toronto, Canada, 2010, pp. 7780-7794

[23]Barker, J. M., and Balas, G. J., "Comparing linear parameter-varying gain-scheduled control techniques for active flutter suppression ", *AIAA Journal of Guidance, Dynamics and Control: Benchmark Active Control Technology Special Section*, Part I, Vol. 23, No. 5, 2000, pp. 948-955.

[24]Gahinet, P., Nemirovski, A., Robust Control Toolbox: LMI Lab, The MathWorks Inc., Natick, MA, 2011.